check for updates

ARTICLE

# Performance Improved of a Lime and Hemp-Based Concrete through the Addition of Metakaolin

Suzanne Daher[*], Amar Benazzouk, Haïkel Ben Hamed and Thierry Langlet

Université de Picardie Jules Verne Avenue des Facultés, Amiens, 80025, France

[*]Corresponding Author: Suzanne Daher. Email: suzie.daher@yahoo.fr

## ABSTRACT

This work describes in detail the experimental investigation of the physico-mechanical properties of nonstructural hemp concrete (usually used as insulating wall material) when the Air-lime based Tradial PF70 binder is partially replaced using Metakaolin. The objective is to reduce the amount of free $Ca^{2+}$ ions in the binder as these are responsible for the degradation of vegetables particles and can therefore induce a loss of mechanical performances. In order to assess the effectiveness of pozzolanic reaction, amounts of 0%, 10%, and 20% vol. of Air-lime binder were replaced by the Metakaolin material, while testing the mechanical properties of concrete specimens containing 200% and 300% of hemp particles. Through SEM and EDX analysis, a tight relationship has been found to exist between the Metakaolin content and physical-mechanical properties of specimen. The pozzolanic reaction consumes calcium hydroxide from binder to produce Hydrated Calcium Silicates (C-S-H) and in turn, this leads to a decrease in the pH-value of the pore solution which is the main factor responsible for hemp particle degradation.

## KEYWORDS

Agro-sourced materials; hemp particles; tradical PF70 binder; metakaolin; pozzolanic products; mechanical properties; deformability; particle mineralisation; SEM and EDX analyses

## 1 Introduction

Building materials based on plant particles are currently considered among the very promising materials, due to renewable resources, their low carbon impact and their hygrothermal performance. However, their problem generally lies in low mechanical strength compared to conventional concretes. Problems related to environmental issues have prompted extensive research into new environmentally friendly building materials. The construction sector is indeed responsible for a high consumption of primary energy and $CO_2$ emissions [1–3]. Therefore, it appears important to develop sustainable building materials with low embodied energy and low carbon emission to replace conventional aggregates, while several products have been already used in construction field to solve environmental and economic problems [4–7].

In this context, particular interest has been given to the use of vegetable particles obtained from renewable sources in composite materials [8,9]. In this respect, some of the important elements are the reduction of the consumption of energy and natural raw materials. A combination of interesting

mechanical and physical properties with their environmental benefit has been the main driver for their use as alternatives for conventional building materials.

The use of renewable raw material derived from vegetable products has been the subject of extensive research. Various types of vegetable by-products (flax, hemp, coir, jute, bamboo, palm…), after being processed, have been used as aggregates and/or fibers replacement of sand and gravels in concrete and mortars [10,11]. The use of these particles is interesting as they exhibit a set of important advantages, such as wide availability at relatively low cost, bio-renewability, ability to be recycled, biodegradability, non-hazardous nature, low carbon footprint, and interesting physical properties (low density, high porosity, hydrophilic nature and high capacity of moisture adsorption). Agro-sourced materials are currently considered among the most promising materials in sustainable engineering technologies due to their many potential applications. In addition to sustainable credential advantage, the use of agro-sourced concretes exhibited high thermohygric performances and provides healthy living environment, due to the vegetable materials ability to regulate indoor humidity buildings [12].

Nevertheless, these new materials are often used as a filling material in construction, and not as load-bearing elements, due to their limited mechanical strengths. In addition, the hydrophilic nature of plant particles leads to a notable decrease in physical, mechanical and thermal properties and eventually rotting due to fungi attack. However, for several decades, several authors have studied the feasibility of improving the thermal, mechanical and physical insulation properties of these composite materials through the use of various types of vegetable materials in aggregates and/or fiber forms including pineapple leaf, date palm, kenaf, Alfa, Diss…,etc, as sand and/or aggregates replacement in concrete and mortars to enhance several properties [13–16]. The results have shown that the specimens exhibited several potential applications such as acoustic and thermal insulation, fire resistance cladding, and the enhancement of flexural strengthening of composite while results in improvement of toughness energy. The properties of composites-based vegetable materials depend on the matrix, particles, and on their interfacial bond. For example, the role of vegetable fibers as reinforcement lies in combining in an adequate manner the proper interfacial bond between the fiber and the matrix. Generally, the adhesion between particles and matrix in composite materials plays an important role in their final mechanical and physical properties.

In the same way, composites based on other vegetable materials such as straw bales, rapeseed straw, corn stalk, jute straw, Diss, and rice husks mixed with different types of binder have found to be energy efficient materials and provide concrete with high performances of thermal insulation [17–20]. Other previous work has shown that the low mechanical strength of agro-sourced materials is in part due to the high water absorption of the particle aggregate and the poor aggregate/binder adhesion [21]. A possible degradation of the plant particles and their bond with the binder therefore poses the problem of the durability of these building materials.

The degradation problem may be due to a weakening of the fibers by alkaline attack, mineralization of the aggregates by the migration of hydration products [22,23]. This causes the material to have a reduction in post-cracking strength and fracture toughness. In order to restrain the degradation of vegetable particles in alkaline medium which is in part responsible for the low vegetable concrete durability, several methods have been studied including particles impregnation with blocking or water repellent agents, sealing of the matrix pores, or reduction of alkalinity [24]. Other studies have also shown the benefits of using natural pozzolan combinations in improvement of mechanical properties of specimens. The reaction occurred between the calcium ions from dissolved Calcium Hydroxide hydrates contained in the hydraulic binder and the amorphous silica, produces a stable components of C-S-H, which are the main responsible for the strength development of specimen [25–28].

The novelty approach in this study consists in a separate investigation of the degradation mechanism of hemp particle under a combination effect of alkali-attack and mineralisation, by analysing the change in the

surface morphology and microstructure modifications. This work also allows the description of the metakaolin addition effect to restrain the particles degradation degree through the reduction in the pH pore solution of the binder medium, while the work reported in the literature investigate only the physic-mechanical properties of the specimen-based hemp particles without considering the environmental medium effect as regards binder-hemp particles interactions.

The aim of this work is to investigate the effect of alternative binder based-Metakaolin on the properties of hemp concrete, while a separate investigation of the physico-chemical interactions between hemp particles and hydraulic binder has been assessed. The objective is to reduce the migration of $Ca^{2+}$ ions from the basic binder towards the hemp particles through the mineralization process, which causes their degradation and thereby a loss of mechanical performances of the specimen. It consists to partial replacement of lime binder amount by Metakaolin material in order to consume the free $Ca^{2+}$ ions derived from Calcium Hydroxide contained in lime binder. The reaction occurred between the calcium ions from dissolved Calcium Hydroxide hydrates and the amorphous silica, contained in Metakaolin, produces stable components of C-S-H, according to the reaction mechanism of:

$$3Ca^{++} + 2H_2SiO_4^{2-} + 2OH^- + 2H_2O \rightarrow Ca_3[H_2Si_2O_7](OH)_2 \cdot 3H_2O$$
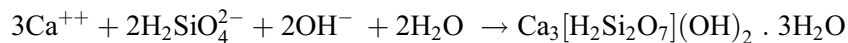
However, investigation of the effect of different amounts of Metakaolin on the neat lime binder has been carried out, while specimens of hemp concrete containing hemp particles for 200% and 300% by volume of the binder were tested.

## 2 Materials and Experimental Testing

### 2.1 Raw Materials

#### 2.1.1 Hemp Particles

Hemp is one of the world's earliest cultivated crops and has a variety of applications including construction. It is one of the most widely used and studied plant particles for the manufacture of building materials. It is cultivated mainly in temperate climate areas. France is the world leader in its culture, although production has fluctuated a lot over the past centuries. The shape of hemp particles used is shown in Fig. 1. Table 1 summarizes the measured properties of these particles and clearly shows that they have a high porosity with, obviously, a high water absorption rate. These particles were also subjected to dimensional analysis with mesh sizes ranging from 0.5 to 15 mm, while the particle sizes distribution is shown in Fig. 2.



**Figure 1:** Shape of hemp particles

**Table 1:** Properties of hemp particles

| Bulk density [kg/m$^3$] | Absolute density [kg/m$^3$] | Porosity [%] | Water absorption [%] |
|---|---|---|---|
| $104 \pm 45$ | $1438 \pm 50$ | $93 \pm 5$ | $290 \pm 15$ |
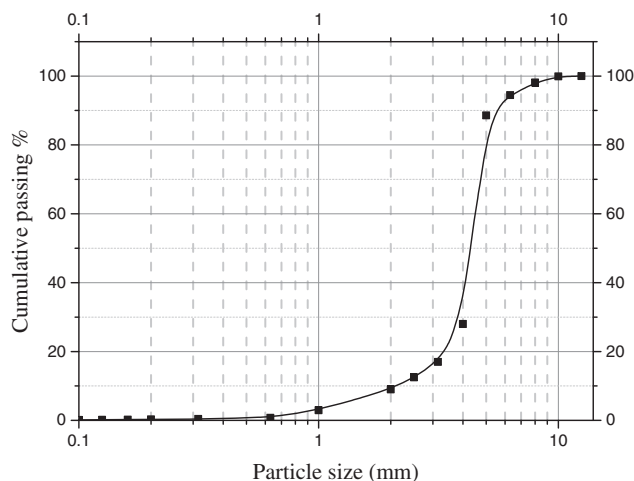


**Figure 2:** Hemp particle size curve

### 2.1.2 Air-Lime-Based Tradical PF70 Binder

The preformulated Air-lime binder (Tradical® PF70) is a mixture of 75% air lime, 10% hydraulic lime and 15% pozzolans, produced by Lhoist industry which is located in the Northern region of France [29]. The basic carbonation reaction of lime leads to the formation of calcium carbonate ($CaCO_3$). The properties of Air-lime based on Tradical PF70 binder are summarised in Table 2.

**Table 2:** Properties of Air lime Tradical PF70-based binder [29]

| Bulk density [kg/m$^3$] | Soluble silica [%] | $CO_2$ content [%] | Adjuvants [%] | Water retention [%] | Maximum grading size [mm] |
|---|---|---|---|---|---|
| $720 \pm 20$ | $10 \pm 2$ | $8 \pm 1$ | $0.5 \pm 0.02$ | $75 \pm 6$ | 0.09 |

### 2.1.3 Metakaolin Material/ARGICAL-M 1000

Metakaolin is a complex amorphous structure obtained after dihydroxylation of clay mineral kaolinite at temperatures between 650°C and 800°C. It is a known admixture for cement-based applications as considered to be more reactive than most other pozzolans. Called ARGICAL-M 1000 and has a chemical formula of $Al_2O_3.2SiO_2$, it is an amorphous non-crystallised material, with a maximum particle size of 0.063 mm It is mainly composed of amorphous silica ($SiO_2$) and alumina ($Al_2O_3$) with an average $SiO_2/Al_2O_3$ mass ratio = 1.2, and can have impurities, mainly quartz. The pozzolanic character of Metakaolin allows it to react with calcium hydroxide ($Ca(OH)_2$) to form Hydrated Calcium Silicate and Hydrated Calcium Silico-Aluminate that achieve higher mechanical strength than Calcium Carbonate [30]. The chemical composition and physical properties of Metakaolin are reported in Table 3.

**Table 3:** Chemical composition and physical properties of Metakaolin pozzolan [31]

| Chemical composition/physical properties | Value |
|---|---|
| $SiO_2$ | 59.00% |
| $Al_2O_3$ | 36.30% |
| $Fe_2O_3$ | 1.40% |
| CaO | 0.10% |
| $MgO_3$ | 0.10% |
| Pozzolanic Activity index (28 days) | 1.03 |
| Specific area (BET) | 20 $m^2/g$ |
| Bulk density | 400 $kg/m^3$ |
| Specific gravity | 2400 $kg/m^3$ |

### 2.2 Samples Formulation

Two types of samples were prepared. The former consist of neat binder without aggregates, in which lime binder was substituted by 10% or 20% by weight of Metakaolin. A second series of samples was then prepared for the hemp concretes where the binder contained 20% of Metakaolin and hemp particles for 200% and 300% by volume of the binder, respectively.

For all samples, Metakaolin and Air-lime based binder were initially mixed in a planetary mixer. The total mixing water added for all specimens corresponds to that used for fresh control mortar in order to achieve the normal workability (as measured by flow test). For the hemp mortars, the plant particles were then slowly and evenly dispersed throughout the binder, and the fresh material was allowed to mix for an additional three minutes. All the specimens were then compacted on a vibrating table and moist-cured for 28 days at 20°C ± 2°C and 98% relative humidity.

The different specimens studied are designated by:

- Tr: Pure lime binder Tradical without Metakaolin;
- TrMK10: Tradical and 10% Metakaolin;
- TrMK20: Tradical and 20% Metakaolin;
- BCT2: Hemp concrete based on pure Tradical by using 200% by volume of hemp particles;
- BCT2MK: BCT2 with 20% Metakaolin;
- BCT3: Hemp concrete based on pure Tradical by using 300% by volume of hemp particle;
- BCT3MK: BCT3 with 20% Metakaolin.

The designation of each formulation as well as its composition is given in Tables 4 and 5.

**Table 4:** Mix-proportions of specimens (Neat binder)

| Specimen-ID | Tradical PF70 [%] | Metakaolin MK [%] | Water/binder ratio | Hemp particles [%] |
|---|---|---|---|---|
| Tr | 100 | 0 | 0.5 | 0 |
| TrMK10 | 90 | 10 | 0.5 | 0 |
| TrMK20 | 80 | 20 | 0.5 | 0 |

**Table 5:** Mix-proportions of specimens (Hemp concrete)

| Specimen-ID | Tradical PF70 [%] | Metakaolin MK [%] | Water/binder ratio | Hemp particles [%] |
| --- | --- | --- | --- | --- |
| BCT2 | 100 | 0 | 1 | 200 |
| BCTMK2 | 80 | 20 | 1 | 200 |
| BCT3 | 100 | 0 | 1.1 | 300 |
| BCTMK3 | 80 | 20 | 1.1 | 300 |

For measurements of hardened properties, prism and cylindrical samples of 70 mm × 70 mm × 280 mm and 110 mm × 220 mm in sizes were prepared, for flexural and compressive tests, respectively. The shapes of different specimens after demolding are shown in Fig. 3.



Cylindrical sample
(110 x 220 mm)

Prismatic sample
(70 x 70 x 280 mm)
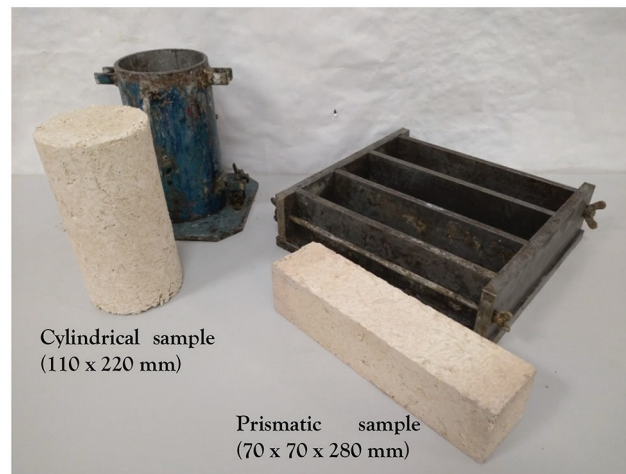
**Figure 3:** Shapes of hardened cylindrical and prismatic specimens

## 2.3 Experimental Testing

### 2.3.1 Mechanical Compressive and Flexural Strengths

The tested properties on the hardened specimens include dry unit weight, as determined by means geometrical measurement and weighting. The compressive tests were carried out on 110 mm × 220 mm cylindrical samples in accordance with Standard EN 196-1 [32], using an electromechanical testing machine SHIMADZU AG-IC model, with 250 kN in load cell. The rates of loading of compressive tests were 4 mm/min (Fig. 4). Three replications were used for each tested property. The compressive stress-strain curves have been recorded to evaluate the variation of ultimate strain, the elastic modulus, and ductile and/or brittle nature of the specimens, namely: the reference mortar (the Tradical PF70 binder, the binder by adding Metakaolin), the hemp concrete based on binder using 200% and 300% by volume of hemp particles without or by adding Metakaolin.

The three-point bending flexural tests were carried out on prismatic specimens of dimensions 70 mm × 70 mm × 280 mm. These tests were carried out in accordance with the Standard EN 196-1 [32]. The press used is of the TINUS OLSEN H50KS type, with a loading capacity of 50 kN. The load is applied at an equal distance from the supports at a speed of 0.4 mm/min, until the material breaks (Fig. 5). By the load-deflection diagrams we evaluate many parameters as flexural strength, ultimate deflection at peak load, elastic modulus of rupture, and ductile and/or brittle nature of the specimens. The flexural strength-values were calculated using Eq. (1)

$$R_f \, (MPa) = \frac{3 \cdot F_f \cdot L}{2bd^2} \tag{1}$$

where, $R_f$ is the strength of the specimen at the plane of failure (MPa); $F_f$ is the maximum load recorded by the testing machine (N); $L$ is the span length (mm); $b$ is the average thickness of the specimen at the failure plane (mm); $d$ is the average depth of the specimen at the plane of failure (mm).
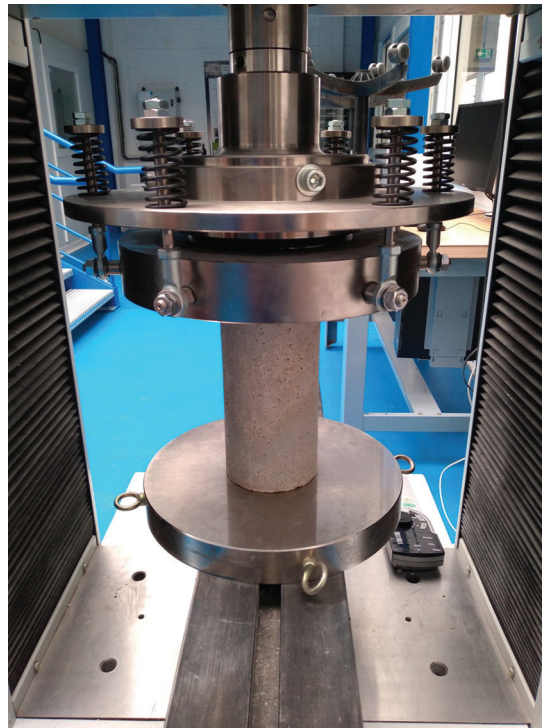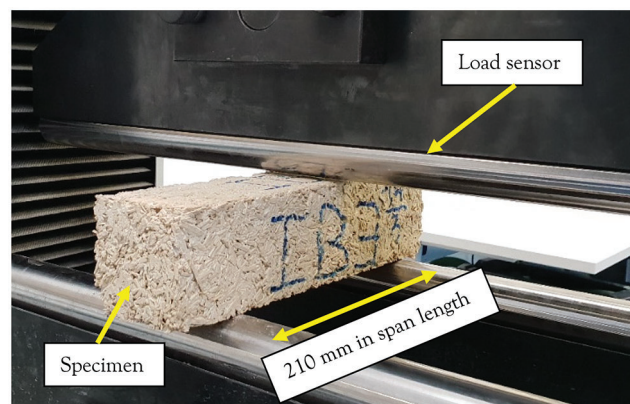


**Figure 4:** Compressive testing machine



**Figure 5:** Three-point bending flexural-tests

As the first part of the stress-strain curves shows à linear quasi-elastic behavior, the initial elastic stiffness is determined from the slope of the curves. The elastic modulus from flexural-test was determined using Eq. (2).

$$E_f = K \frac{L^3}{48\,I} \tag{2}$$

where $E_f$ is the elastic modulus (MPa); $K$ is the elastic stiffness (N/mm), which represents the slope of the linear part of load-deflection curve; $I$ (mm$^4$) is the sample inertia.

A first approach to evaluate the effect of fiber addition on specimen toughness is to measure the amount of energy to be applied to the material to realize total failure in the compressive and flexural strength tests, respectively. The value of the tenacity was obtained by calculating the total area under the stress-strain diagram for the compressive test and the load deflection curve for flexural-test.

### 2.3.2 Physico Chemical Interactions Binder/Aggregates

The influence of the alkaline medium on the hemp aggregates was analyzed by scanning electron microscopy (SEM). A scanning electron microscopy (SEM) Environmental Quanta 200 FEG type was used to study the structure of the binder, the vegetable particles and their bonding to the matrix. Before the SEM analysis, a carbon metallization step is necessary to increase the conductivity and allow quality images to be acquired. The technical characteristics are as follows: resolution from 1 nm to 15 kV; low energy allowing to have an almost monochromatic beam; samples up to 50 mm in diameter.

For the observations on the hemp particles, they were first immersed in a binder-based solution with or without Metakaolin. In order to homogenize the mixtures, the aggregates were stirred for 48 h using a magnetic stirrer then the aggregates were rinsed with demineralized water and then dried. The observations were made first on the outer surface of the hemp particles, then, after cutting them on the cross section. In a second phase, we recovered hemp particles after bending tests on concrete specimens, and observed the particles directly using SEM micrograph analyses.

### 2.3.3 Energy-Dispersive X-ray Spectroscopy EDX

In order to complete the observations made by scanning electron microscopy, X-ray analyzes (EDX) were carried out on the binder and the hemp aggregates. This EDS analysis makes it possible to determine the concentration of $Ca^{2+}$ ions present in the binder itself and in the aggregates after immersion in the binder-based solution.

### 2.3.4 pH Measurement

The purpose of this measurement is to determine the degree of alkalinity of Air-lime based binder with an without Metakaolin addition. The pH-variation was assessed throught the measurement of the pore solutions by a pH-electrode, using the suspension method [33]. After crushing and sieving to 3/5 mm in size, 100 g of the sample aggregates were mixed and continuously stirred with distilled water for 12 h. Before pH-measurements, the aqueous solution was vacuum filtered using two filter papers with 30 and 15 μm in pore size, respectively, to remove the rest of suspended particles. The pore solution of Tr, TrMK10 and TrMK20 samples were prepared, while the pH-measurement device are shown in Fig. 6.

## 3 Experimental Results and Discussion

The physico-mechanical properties of hardened mortars specimens were tested at 28-days. Three types of samples were tested: the Tradical lime binder alone (Tr), lime binder with 10% and 20% Metakaolin (TrMK10 and TrMK20); their composition has been given in Table 5.

**Figure 6:** pH measurement procedure

## 3.1 Characteristics of the Binder

### 3.1.1 Influence of Metakaolin on the Compressive Strength of the Binder

The objective of this part is to investigate the effect of Metakaolin addition on the strengthening of mechanical properties of neat Air-lime Tradical binder over time. Metakaolin amount was varied from 0% to 20% vol. in order to assess the pozzolanic activity which refers to the degree of reaction over time occurred between a pozzolan and $Ca^{2+}$ ions from dissolved calcium hydroxide($Ca(OH)_2$). Based on the works conducted by Wei et al. [32] on the durability-study of hem concrete, the use of Metakaolin amount higher than 20%, will generates the adverse effect. The authors concluded that the higher amount of free amorphous silica ($SiO_2$) without reacting due to the low free $Ca^{2+}$ ions in medium binder affects negatively the mechanical properties of sample. The variation of compressive strength *vs.* curing time is shown in Fig. 7. It should be noted that the compressive strength increased *vs.* time regardless Metakaolin percentage, while the higher pozzolanic activity is achieved during the first 28-day of curing time. For longer curing time, the pozzolanic reaction degree becomes approximately constant. The 28-day strength values are listed in Table 6 and they are approximately 5.1 MPa for Tr without Metakaolin, 6.0 MPa for TrMK10 and 7.2 MPa for TrMK20. Compared to the compressive strength of Tr, the strengthening is respectively 18% for TrMK10% and 41% for TrMK20 higher than he sample without Metakaolin addition.
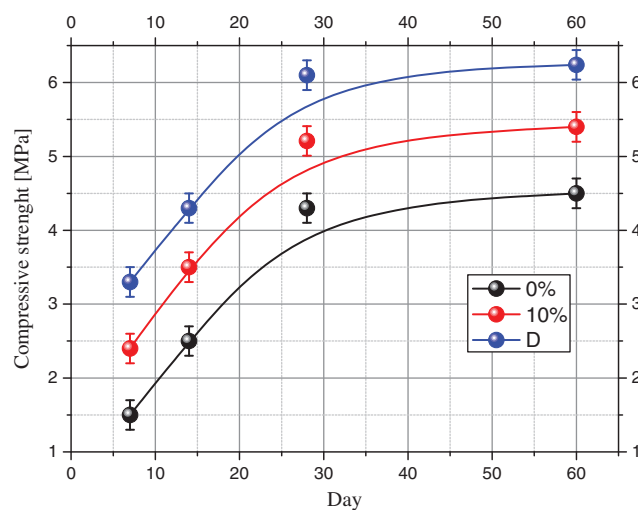


**Figure 7:** Effect of Metakaolin content on the compressive strength of binder *vs.* time

**Table 6:** Compressive strength of binder with and without Metakaolin at 28 days

| Specimen-ID | Dry unit density [kg/m$^3$] | Compressive strength [MPa] | Ultimate strain [mm/m] | Elastic modulus [MPa] |
|---|---|---|---|---|
| Tr | $840 \pm 20$ | $5.1 \pm 0.5$ | $4.43 \pm 0.6$ | $1343 \pm 15$ |
| TrMK10 | $854 \pm 25$ | $6.01 \pm 0.7$ | $5.85 \pm 0.3$ | $1382 \pm 25$ |
| TrMK20 | $872 \pm 40$ | $7.2 \pm 0.4$ | $4.90 \pm 0.5$ | $1453 \pm 20$ |

### 3.1.2 Influence of Metakaolin on the Flexural Strength of the Binder

The flexural tests were carried out on prismatic samples of 70 mm × 70 mm × 280 mm in size. The obtained results after 28 days are reported in Table 7. It can be observed that the flexural strength increased by 7.4% and 14.2% for 10% and 20% of Metakaolin, respectively. However, the increase in flexural strength is lower than that in compressive strength. It is therefore evident that pozzolanic reaction should contribute to enhance mechanical strength of specimen due to the production of additional C-S-H hydrates. In addition, the increase in amount of pozzolanic products also leads to fill the pores and thereby reduces the porosity of the matrix.

**Table 7:** Flexural strength of binder with and without Metakaolin at 28 days

| Specimen-ID | Load (N) | Flexural strength (MPa) | Ultimate deflection (mm) |
|---|---|---|---|
| Tr | $1412 \pm 20$ | $1.48 \pm 0.10$ | $0.14 \pm 0.02$ |
| TrMK10 | $1518 \pm 10$ | $1.59 \pm 0.25$ | $0.18 \pm 0.02$ |
| TrMK20 | $1607 \pm 8$ | $1.69 \pm 0.20$ | $0.16 \pm 0.03$ |

### 3.1.3 Effective Influence of Metakaolin

The previous results show that the partial replacement of lime binder by Metakaolin enhances the mechanical performances of the binder matrix. The reaction occurred between metakaolin and $Ca(OH)_2$ generates new products of C-S-H and Alumino-Silicates hydrates which are considered as the main components for the binder strengthening. Fig. 8a shows the SEM observations of the neat binder which indicates abundant free $Ca(OH)_2$ hydrates needle shaped. In contrast, the binder containing 20% of Metakaolin is largely hydrated, resulting in a production of high amount of C-H-S hydrates (Fig. 8b).
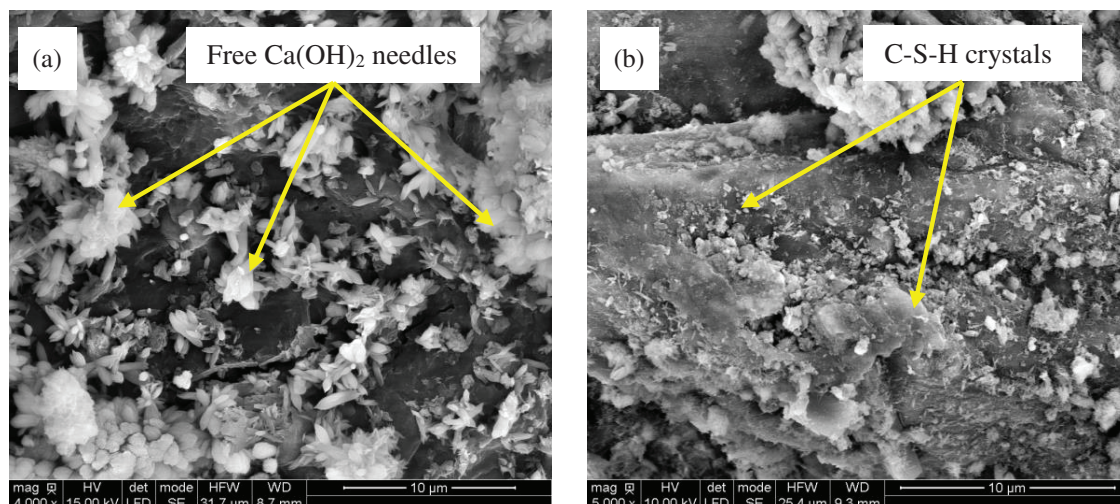


**Figure 8:** SEM-images for binders: (a) Neat Tr, (b) TrMK20

To understand this effect, we observed a section of the material with a scanning electron microscope. From these observations, one notes a greater formation of C-S-H crystal hydrates in the presence of 20% of Metakaolin (Fig. 8a) which improve the mechanical performances of the binder, compared to the neat lime binder (Fig. 8b). To confirm this analysis, an EDX analysis gives the diphractograms of Fig. 9. For the lime binder alone, there is a large deposit of $Ca^{2+}$ ions while in the presence of Metakaolin, the deposit is weaker. This confirms the pozzolanic character of Metakaolin which reacts with the calcium hydroxide present in hydraulic lime, and contributes to consuming more $Ca^{2+}$ ions during the hydration of the binder.
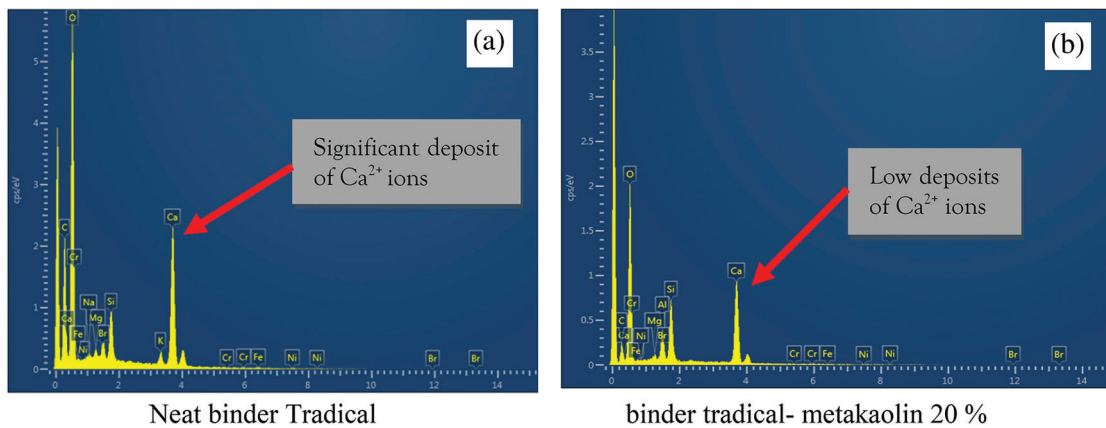


Figure 9: EDX diffractogram analyses

After having crushed the test pieces, they are diluted in water, we found that the pH of the solution decreases *vs.* in the percentage of Metakaolin (Table 8). This alkalinity decrease in the solution can be explained by a decrease in free $Ca^{2+}$ ion. Thus, as observed by [18,19], the pozzolanic character of Metakaolin contributes to increase the mechanical strength of a lime binder. In the remainder of this work, the base binder will be replaced only by 20% metakaolin.

Table 8: pH-value as a function of MK percentage

| pH (Tr) | pH (Tr+10% MK) | pH (Tr+20% MK) |
|---|---|---|
| $12.2 \pm 0.2$ | $12 \pm 0.1$ | $11.7 \pm 0.1$ |

### 3.2 Characteristics of Specimens

The hemp concrete studied is based on Tradical without or with 20% of Metakaolin and includes 200% and 300% volumes of hemp particles, respectively BTC2 and BTC2MK or BTC3 and BTC3MK. The materials are formulated from the composition of a conventional mortar composed of a binder in which vegetables particles have been incorporated at volume contents of 200% and 300% for hemp, with a Water/Binder ratio close to 1. For each formulation the results are compared with the ones of the binder alone, Tr and TrMK. Compressive and flexural strength measurements are performed with the same press as in the previous section.

#### 3.2.1 Dry Density of Specimen

Apparent density-value of dry hemp concrete at different hemp volumes is shown in Fig. 10. The hardened unit dry weight value decreases as the vegetable particle amount increases. With 300% volume of hemp particles, the density of the initial binder is almost divided by 2, with or without metakaolin. For

hemp concrete, the density decreases by about 20% when the volume content of hemp particles increases from 200% to 300%, and for both formulations is 6% higher in the presence of metakaolin. It reaches respectively 420 kg/m$^3$ and 445 kg/m$^3$ for BCT3 and BCT3MK. The specimen lightening is related to the physical properties of hemp particles, since they exhibited lower density than binder matrix. The addition of vegetable particles leads to reduce the compactness of specimen, thus allowing to increase the porosity which contributes to lightening the sample. However, the lower lightening rate of specimen with metakaolin addition is probably related to the matrix densification due to the additional production of hydrate components (C-S-H). These hydrates could be effective in the reduction of the matrix porosity and also in the improvement of the interfacial transition zone (ITZ) between vegetable particles and binder matrix.
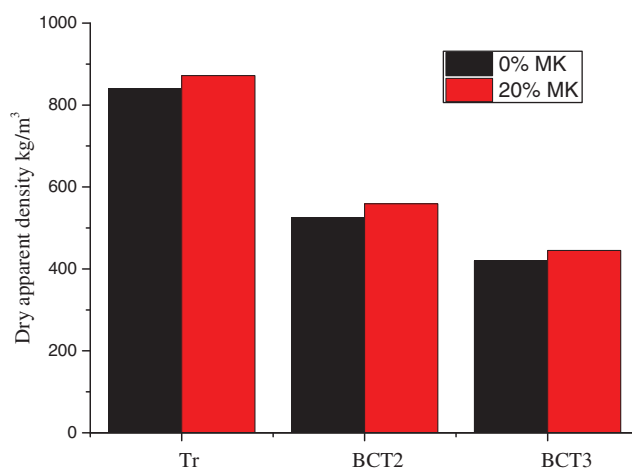


**Figure 10:** Apparent density of dry composite at different fiber volumes

### 3.2.2 The Influence of Hemp Particles on the Compressive Strength

The Tr, TrMK (20%), BCT2, BCT2MK, BCT3, BCT3MK specimens were tested along 28-days and the results, including ultimate strain and elastic moduli, are listed in Table 9.

**Table 9:** Mechanical properties of different specimen under compressive-test at 28-days

| Specimen-ID | Dry unit weight [kg/m$^3$] | Compressive strength [MPa] | Ultimate strain [mm/m] | Elastic modulus [MPa] |
|---|---|---|---|---|
| Tr | $840 \pm 10$ | $5.10 \pm 0.5$ | $4.43 \pm 0.5$ | $1343 \pm 20$ |
| TrMK (20) | $872 \pm 15$ | $7.20 \pm 0.6$ | $4.9 \pm 0.7$ | $1453 \pm 5$ |
| BCT 2 | $525 \pm 18$ | $1.52 \pm 0.2$ | $51 \pm 2$ | $138 \pm 8$ |
| BCT2MK | $559 \pm 10$ | $1.71 \pm 0.1$ | $60 \pm 1.5$ | $144 \pm 5$ |
| BCT3 | $420 \pm 20$ | $0.29 \pm 0.08$ | $132 \pm 6$ | $62 \pm 2$ |
| BCT3MK | $445 \pm 20$ | $0,42 \pm 0.05$ | $188 \pm 5$ | $78 \pm 2$ |

As already seen with the neat binder, replacing part of Tradical with Metakaolin increases the compressive strength of the hemp concrete, whether for 200% and 300% volumes of plant particles. At the same time, it can be seen that increasing the hemp particle content in the mortar increases the ultimate strain value, which induces higher ductility of the specimen. However, the loss in mechanical strength is

significant when the rate of plant particles is increased, i.e., on average nearly 80% between BCT2-BCT2MK and BCT3-BCT3MK. It is obvious that the mechanical compressive strength is correlated to the concrete density. In addition, this decrease in compressive strength can be related to porous structure of sample. The more the air-voids ratio, the lighter the specimen and the lower its mechanical strengths.

The typical variations and the corresponding mean values of the peak stress, strain, and elastic modulus for all specimens are shown in Fig. 11. The effect of adding hemp particles to the binder leads to increase the ultimate strain value, which induces higher ductility of the specimen.
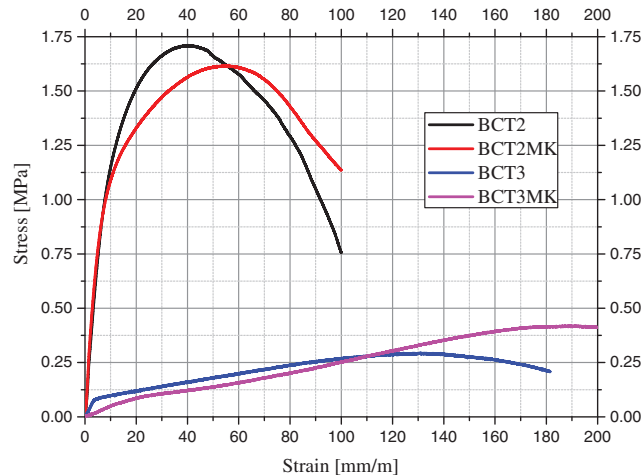


**Figure 11:** Stress-strain diagrams of hemp concrete specimens

The BCT2 and BCT2MK specimens exhibit a ductile failure; the ultimate strain-value varied from 51 mm/m for BCT2 to 60 mm/m for BCT2MK. Despite a low level in compressive strength, samples BCT3 and BCT3MK show the same mechanical behavior, with a more extended plastic phase and a larger strain before failure, respectively 132 mm/m and 188 mm/m for BCT3 and BCT3MK.

It is interesting to examine the in failure mode change of specimens after reaching a maximum load. Fig. 12 leads to compare the failure shape of hemp concrete and the neat binder specimen in post-cracking phase. It can be shown that the neat binder sample exhibits a brittle failure characterized by vertical cracks and sudden fracture, resulting in shattering into small pieces. In contrast, the hemp concrete specimen experienced a ductile failure mode and was able to support loads after reaching its maximum capacity. This failure mode can be explained by the ability to withstand large plastic deformation before fracture. The failure of hemp concrete without disintegration and its capacity to sustain load in post-failure phase could be related to the bridging effect of cracks by hemp particles. The higher deformability and the ductile failure combination lead to restrain a risk of cracking of specimen when post-cracking phase is attained. Similar behavior has been observed by several authors when vegetable materials were used as mineral aggregates replacement in concrete-based different binder types [34,35].
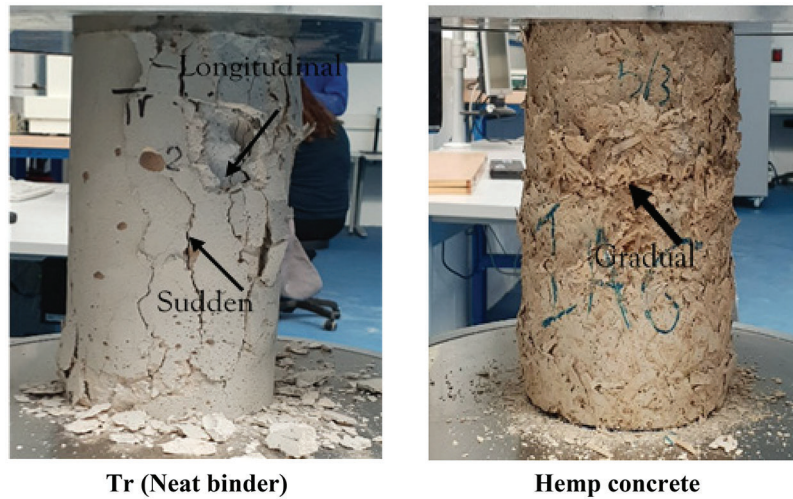
**Tr (Neat binder)**          **Hemp concrete**

**Figure 12:** Specimen shapes after failure under compressive test

### 3.2.3 The Influence of Hemp Particles on the Flexural Strength

The Load-deflection diagrams obtained under three binding-tests of all specimens are reported in Fig. 13, while the corresponding parameters-values are shown in Table 10. It can be observed that, unlike the response of control specimens (Tr and TrMK) characterized by a purely elastic phase before localization of the rupture, the presence of hemp particles let appear a plastic deformation which characterizes the improvement of the ductile behavior of the composite.
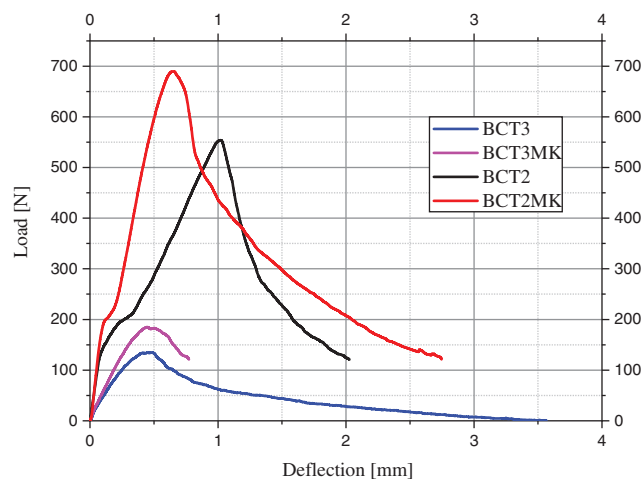


**Figure 13:** Load-deflection diagram for different specimens

As reported in Table 10, a reduction in the flexural strength of the specimen is observed as the hemp particle was added to the lime binder Tradical. Value decreases from 1.48 MPa for Tr specimen to 0.58 MPa for BCT2 specimen. It corresponds to reduction of up to 60%. In the same way, the loss in flexural strength is significant when the rate of plant particles is increased, i.e., on average nearly 61% between BCT2-BCT2MK and BCT3-BCT3MK. As for the compression tests, replacing part of Tradical by Metakaolin increases the flexural strength of the hemp concrete, but only by 24% and 35%, respectively

for 200% or 300% by volume of hemp particles. The flexural strength reduction observed is due to both mechanical properties of hemp particles and porous structure of the matrix effect.

**Table 10:** Mechanical properties of different specimen under flexural-test at 28-day

| Material mix | Load [N] | Flexural strength [MPa] | Ultimate deflection [mm] | Elastic modulus [MPa] |
|---|---|---|---|---|
| Tr | $1412 \pm 20$ | $1.48 \pm 0.1$ | $0.12 \pm 0.01$ | $1323 \pm 15$ |
| TrMK20 | $1607 \pm 25$ | $1.69 \pm 0.2$ | $0.16 \pm 0.02$ | $1438 \pm 10$ |
| BCT 2 | $553.9 \pm 12$ | $0.58 \pm 0.05$ | $0,97 \pm 0.03$ | $123 \pm 10$ |
| BCT2 MK | $689.6 \pm 15$ | $0.72 \pm 0.08$ | $0.68 \pm 0.03$ | $169 \pm 12$ |
| BCT3 | $135.2 \pm 10$ | $0.14 \pm 0.05$ | $0.47 \pm 0.01$ | $54 \pm 5$ |
| BCT3 MK | $185.3 \pm 24$ | $0.19 \pm 0.02$ | $0,44 \pm 0.02$ | $73 \pm 3$ |

During the tests, a bridging phenomenon was observed for materials based on hemp particles, making it possible to delay the propagation of cracks. Fig. 14 shows photographs of the materials after failure. Unlike the control specimen (Tr), those based on vegetable particles retain their structure, keeping the lips of the crack linked, "stitched". The latter therefore make it possible to better control the propagation of cracks, thus delaying the failure phase.
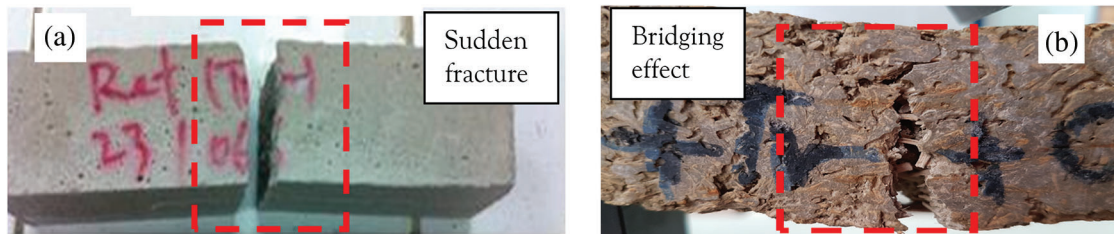


**Figure 14:** Failure mode of specimens, after bending test. (a) Control specimen (Tr)-sudden failure; (b) Hemp specimen-bridging effect

### 3.2.4 Elasticity Behavior Change

It is noted that the behavior of the reference material (Tr) is characterized by a short elastic phase, followed by a sudden rupture. For this control specimen, the breaking is sudden and rapid, without plastic zone. On the other hand, the presence of vegetable particles gives the material a behavior in a linear behavior until the load recovery, then by the appearance of a very marked non-linearity, followed by a ductile and flexible behavior, with the absence of post-peak. However, despite an unfavorable impact on compressive strengths, the presence of vegetables particles improves the elastic behavior of specimen.

The brittle or ductile behavior of specimens has been also characterized by evaluating the Brittleness Index (BI), using hysteresis loops, obtained during the loading/unloading cycle. *BI*-value was estimated through the ratio between stored elastic energy ($A_2$) and dissipated plastic energy ($A_1$) [35]. As indicated in Fig. 15, the energies ($A_2$) and ($A_1$) were evaluated from the areas under the hysteresis loops, as the average values of three replications cycles for each specimen. If the ratio is close to zero, all energy is irreversible and the material exhibited ductile behavior. When the ratio tends to infinity, the energy becomes reversible and the material is brittle.
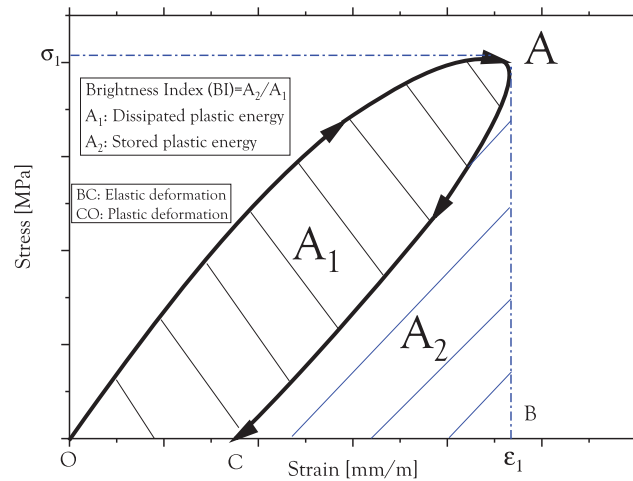
**Figure 15:** Schematic diagram of Brittleness Index evaluation [35]

The stress-strain hysteresis loops obtained for the hemp concretes (BCT2, BCT2MK, BCT3 and BCT3MK), corresponding to 200% and 300% volumes of hemp particles are shown in Figs. 16 and 17. The corresponding Brittleness Index-values of the reference neat Tr and TrMK specimens were reported in Table 11. The results clearly show that the BCT2 and BCT3 materials exhibit greater flexibility, compared to the Tr sample, due to the difference in morphology between the vegetable particles and the binders. As observed previously, these materials exhibit ductile behavior, characterized by a low value of Brittleness Index of 2.1 and 1.43 for BCT2 and BCT3 samples, respectively). For a specimen-based Tr matrix, the high value of Brittleness Index ($BI = 7.9$), makes the specimen brittle.
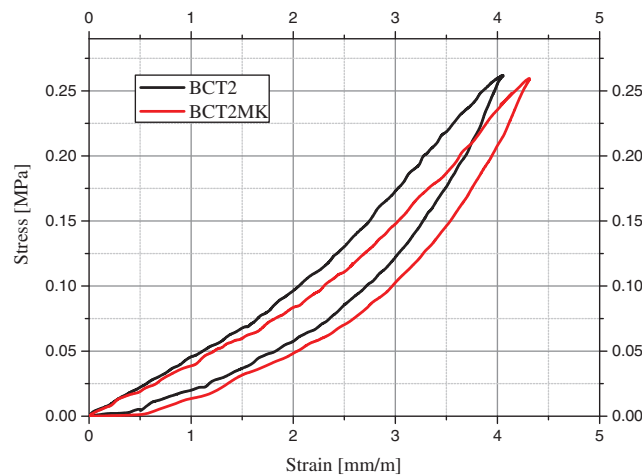


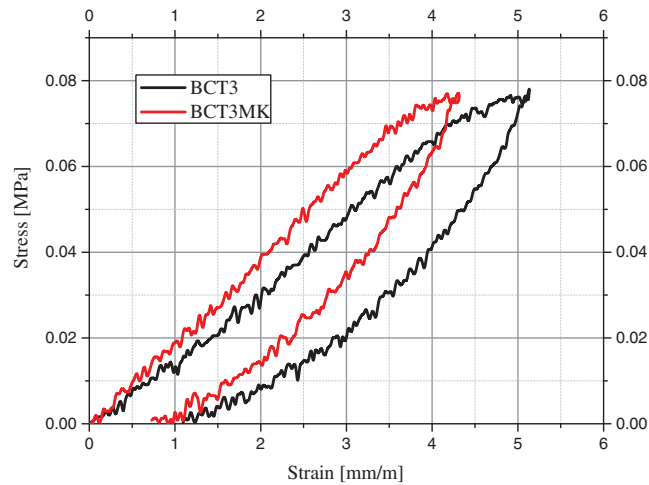**Figure 16:** Hysteresis loops of concrete with 200% volume of hemp particles

**Figure 17:** Hysteresis loops of concrete with 300% volume of hemp particles

**Table 11:** Brittleness index-value of specimens at 28-day

| Specimen-ID | Brittleness Index-value |
|---|---|
| Tr | $7.9 \pm 1$ |
| TrMK | $9.1 \pm 0.8$ |
| BCT 2 | $2.1 \pm 0.2$ |
| BCTMK2 | $2.4 \pm 0.3$ |
| BCT3 | $1,43 \pm 0.08$ |
| BCTMK3 | $1,9 \pm 0.05$ |

### 3.2.5 Physico Chemical Interactions Binder/Aggregates

As described in Paragrap 2.3.2, the hemp particles were immersed in a neat binder solution with and without Metakaolin, while the sections of the aggregates were then analyzed using a SEM micrographs. On the basis of the tests on the surfaces of hemp particles, the ones not immersed in the solution have homogeneous microstructures with a smooth surface (Fig. 18a), while the hemp aggregates immersed in a binder solution have a less smooth surface (Figs. 18b and 18c). In the latter cases, a fixation of calcium nodules on the surface of the hemp particles is observed, which constitutes a discontinuous and random deposit. The concentration of these deposits differs from one solution to another. The aggregates immersed in clear Tradical solution show a significant concentration of $Ca^{2+}$ deposits (Fig. 18b), while the concentration of deposits on those immersed in TrMK solution is less significant (Fig. 18c).

In the same way, we can examine the cross-section of plant particles. It is noted that the raw fiber has an imperfect polygonal section with a central hole: the lumen (Fig. 19a). In comparison, the fiber bundles appear less regular after immersion in the binder solution (Figs. 19b and 18c). As before, there is less deposition of $Ca^{2+}$ ions in the presence of Metakaolin in the solution (Fig. 19c).
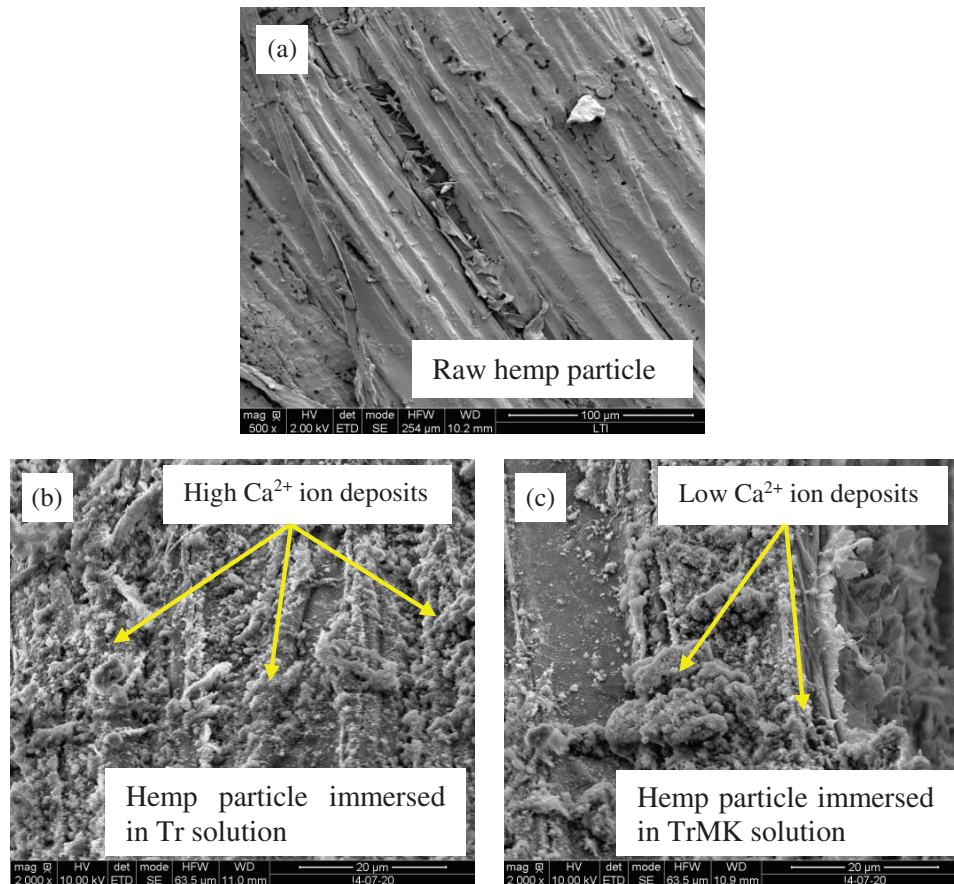
**Figure 18:** SEM micrographs of a longitudinal section of hemp particle

The same observation can be made from plant aggregates recovered after grinding a hemp concrete based on (Tr) and (TrMk) binder. As shown in Fig. 20, it can be observed that the calcium nodule deposits on the surface of hemp particles are less important for the binder containing Metakaolin (Fig. 20b), compared to that with neat (Tr) (Fig. 20a). This finding is important for the durability of the material over time, as $Ca^{2+}$ ions contribute to the degradation of the hemp particles.

These results are confirmed by EDX (X-ray dispersive energy). We notice that there is a decrease in calcium concentration of about 41% when Metakaolin is added. X-ray analysis shows important peak of $Ca^{2+}$ ions in the case of neat Tradical binder (Fig. 21a). The deposit observed on the particles is therefore calcium hydroxide formed by the combination of $Ca^{2+}$ ions, oxygen and hydrogen in the cell walls of the hemp particles. In the presence of Metakaolin the calcium peak is lower (Fig. 21b). Only part of the $Ca^{2+}$ ions reacted with the oxygen and hydrogen in the cell walls of the particles, the other part reacted with the pozzolan (silicon dioxide) to form hydrated calcium silicate.
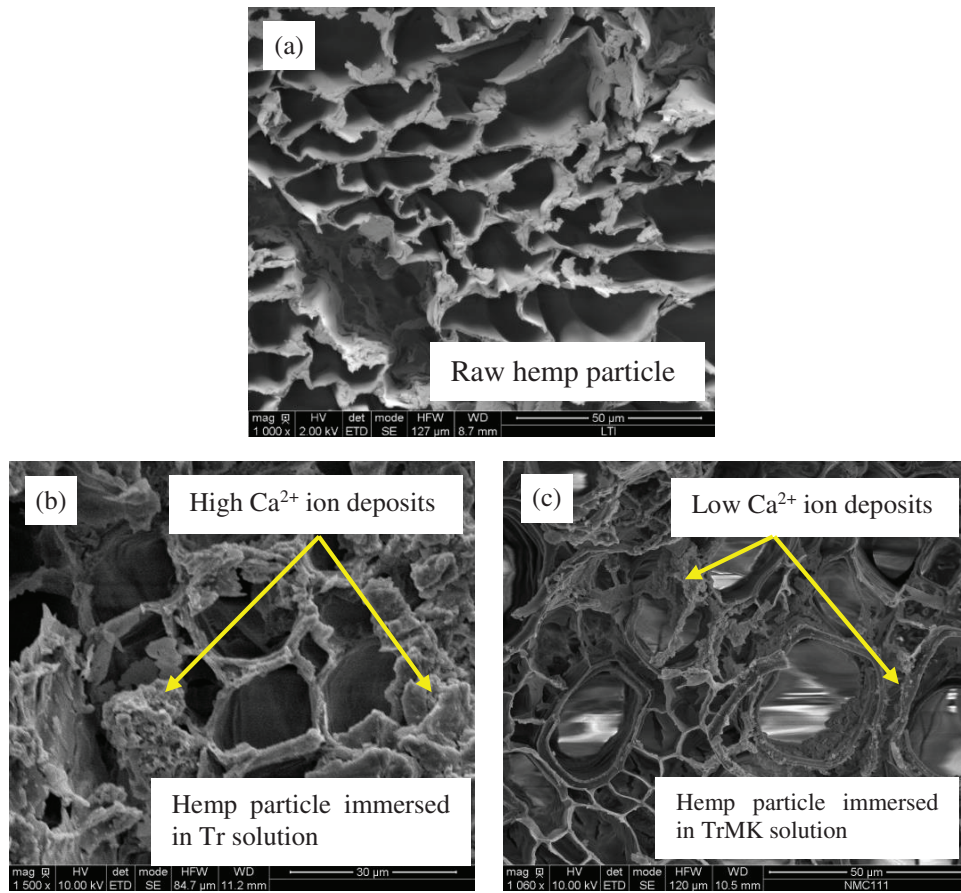
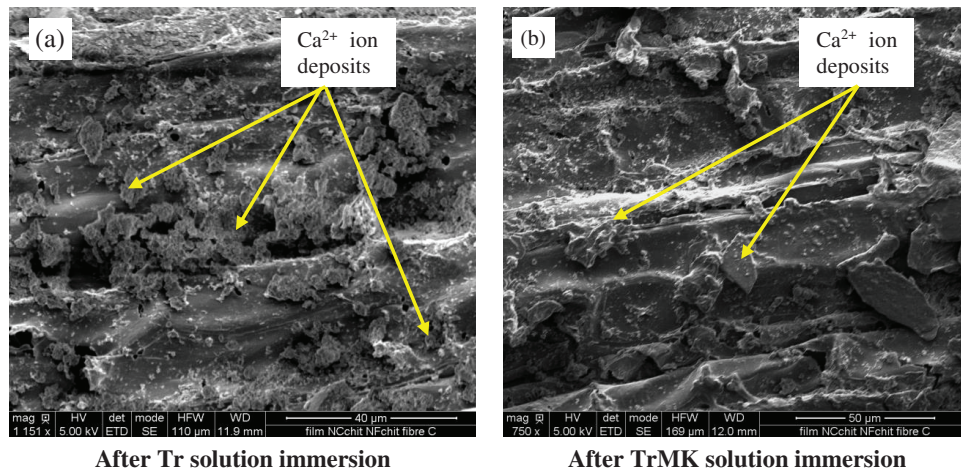**Figure 19:** SEM micrographs of a cross section of hemp particle



**Figure 20:** SEM Micrographs of longitudinal hemp particle section, immersed in a solution

(a) Immersed in Tr solution                          (b) Immersed in TrMK solution
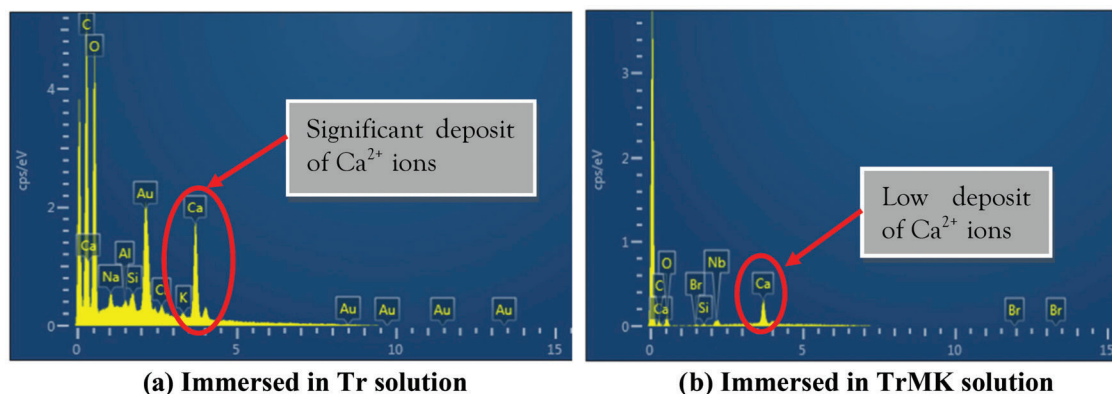
**Figure 21:** EDX analyses of hemp particles after immersion in a binder solution

## 4  Conclusion

This work deals with the investigation of effective means to enhance the mechanical properties of hemp concrete based on Air-lime binder. The objective consists to restrain the hemp particles degradation occurred along time due to the combination effect of alkaline attack and mineralization process, which is considered as the main factor leading to decrease the mechanical strengths of specimen. The investigation was carried out by testing the mechanical properties of hemp concrete containing 20% of Metakaolin as partial replacement of Air-lime binder, while the results have been compared to the usually specimen produced without Metakaolin.

The effectiveness of used Metakaolin on the strengthening of Air-lime binder was separately investigated by evaluating the effect of several amounts of Metakaolin (0%, 10%, and 20% vol.) as partial binder replacement on the mechanical properties. The test-results have shown that the increase of Metakaolin amount enhances the mechanical performances of binder, due to the pozzolanic reaction which produces additional amounts of C-S-H hydrates. For 20% of Metakaolin replacement, the specimen exhibited 41% and 14% greater compressive and flexural strengths, respectively, than the sample without Metakaolin. The SEM micrograph analyses of hydrated components of binder have shown that the Air-lime containing Metakaolin is largely hydrated to produce a high amount of C-S-H hydrates. In contrast, abundant free $Ca(OH)_2$ hydrates needle shaped have been observed for binder without Metakaolin. The X-ray analyses have shown that the low content-value of free $Ca^{2+}$ ions means that a large part of these ions has been reacted with amorphous silica from Metakaolin to produce C-S-H crystals, which are the primarily responsible for the strength development of air lime binder. These results highlighted the capability of Metakaolin to consume free $Ca^{2+}$ ions, and to make the embedded hemp particles less vulnerable.

In the second part, the efficiency of Metakaolin addition on the performances of hemp concrete containing 200% and 300% by volume of vegetable particles has investigated. The results have shown that the addition of 20% vol. of Metakaolin increases the mechanical strength, compared to the hemp concrete with neat Air-lime binder. However, despite the decrease of 20% in dry density of hemp concrete for hemp particles ranged from 200% to 300%, the compressive strength level increased by approximately 80%. It should be noted, that the presence of hemp particles results in ductile behavior of specimen, characterized by the low Brittleness Index-value. As observed in post-cracking shape of specimen, this trends leads to maintain the structure of the material, thus delaying the failure phase and subsequently increasing its safety.

It is concluded that the combination of Metakaolin and Air-lime binder appears to enhance the mechanical strengths of hemp concrete, due to the production of additional C-S-H hydrates and also to the protective effect of hemp particles occurred as regards the mineralization mechanism and alkali-attack.

## References

1.  González, M. J., Navarro, J. G. (2006). Assessment of the decrease of $CO_2$ emissions in the construction field through the selection of materials: Practical case study of three houses of low environmental impact. *Building and Environment, 41(7),* 902–909. DOI 10.1016/J.BUILDENV.2005.04.006.

2.  Diana, V., Aleksandra, N. (2008). Potentials and cost of carbon dioxide mitigation in the word's buildings. *Energy Policy, 36(2),* 642–661. DOI 10.1016/j.enpol.2007.10.009.

3.  Seyfang, G. (2003). Environmental mega-conferences–From Stokholm to Johannesburg and beyond. *Global Environmental Change, 13(3),* 223–228. DOI 10.1016/S0959-3780(03)00006-2.

4.  Khalilpasha, M. H. (2012). Sustainable development using recyclable rubber in self-compacting concrete. *Third International Conference on Construction in Developing Countries (ICCIDC–III),* "*Advancing Civil, Architectural and Construction Engineering & Management*", Bangkok, Thailand.

5.  Sadeghi-Nik, A., Bahari, A., Khorshidi, Z., Gholipur, R. (2012). Effect of lanthanum oxide on the bases of cement and concrete. *Third International Conference on Construction in Developing Countries,* "*Advancing Civil, Architectural and Construction Engineering & Management*", Bangkok, Thailand.

6.  Mousavi, M. A., Sadeghi-Nik, A., Baharia, A., Jind, C., Ahmede, R. et al. (2021). Strength optimization of cementitious composites reinforced by carbon nanotubes and Titania nanoparticles. *Construction and Building Materials, 303,* 124510. DOI 10.1016/j.conbuildmat.2021.124510.

7.  Bahari, A., Sadeghi-Nik, A., Shaikh, F. U. A., Sadeghi-Nik, A., Cerro-Prada, E. et al. (2021). Experimental studies on rheological, mechanical and microstructure properties of self-compacting concrete containing perovskite nanomaterial. *Structural Concrete,* 1–15. DOI 10.1002/suco.202000548.

8.  Sassoni, E., Manzi, S., Motori, A., Montecchi, M., Canti, M. (2014). Novel sustainable hemp-based composites for napplication in the building industry: Physical, thermal and mechanical characterization. *Energy and Buildings, 77,* 219–226. DOI 10.1016/j.enbuild.2014.03.033.

9.  Barra, B., Bergo, P., Alves, C., Savastano, H., Ghavami, K. (2012). Effects of methane cold plasma in sisal fibers. *Key Engineering Materials, 517,* 458–468. DOI 10.4028/www.scientific.net/KEM.517.458.

10. Mohr, B. J., Nanko, H., Kurtis, K. E. (2005). Durability of kraft pulp fiber–cement composites to wet/dry cycling. *Cement and Concrete Composites, 27(4),* 435–448. DOI 10.1016/j.cemconcomp.2004.07.006.

11. Aamr-Daya, E., Langlet, T., Benazzouk, A., Quéneudec, M. (2008). Feasibility study of lightweight cement composite containing flax by-product particles: Physico-mechanical properties. *Cement and Concrete Composites, 30(10),* 957–963. DOI 10.1016/j.cemconcomp.2008.06.002.

12. Jones, D., Brischke, C. (2017). *Performance of bio-based building materials (Woodhead Publishing Series and Structural Engineering).* UK: Woodhead Publishing.

13. Ajouguim, S., Talibi, S., Djelal-Dantec, C., Hajjou, H., Waqif, M. et al. (2021). Effect of Alfa fibers on the mechanical and thermal properties of compacted earth bricks. *Materials Today: Proceeding, 37,* 4049–4057. DOI 10.1016/j.matpr.2020.07.539.

14. SaravanaKumar, M., Kumar, S. S., Babu, B. S., Chakravarthy, C. H. N. (2021). Influence of fiber loading on mechanical characterization of pineapple leaf and kenaf fibers reinforced polyester composites. *Materials Today: Proceedings, 46,* 439–444. DOI 10.1016/j.matpr.2020.09.804.

15. Saghrouni, Z., Baillis, D., Jemni, A. (2020). Composites based on Juncus maritimus fibers for building insulation. *Cement and Concrete Composites, 106,* 103474. DOI 10.1016/j.cemconcomp.2019.103474.

16. Sellami, A., Merzoud, M., Amziane, S. (2013). Improvement of mechanical properties of green concrete by treatment of the vegetable fibers. *Construction and Building Materials, 47,* 1117–1124. DOI 10.1016/j.conbuildmat.2013.05.073.

17.  Lu, Z., Zhao, Z., Wang, M., Jia, W. (2016). Effects of corn stalk fiber content on properties of biomass brick. *Construction and Building Materials, 127,* 11–17. DOI 10.1016/J.CONBUILDMAT.2016.09.141.

18.  Araya-Letelier, G., Antico, C., Burbano-Garcia, C., Concha, J., Norambuena-Contreras, J. et al. (2021). Experimental evaluation of adobe mixtures reinforced with jute fibers. *Construction and Building Materials, 276,* 122127. DOI 10.1016/j.conbuildmat.2020.122127.

19.  Saloni, P., Lim, Y. Y., Pham, T. M. (2021). Influence of portland cement on performance of fine rice husk ash geopolymer concrete: Strength and permeability properties. *Construction and Building Materials, 300,* 124321. DOI 10.1016/j.conbuildmat.2021.124321.

20.  Sheridan, J., Sonebi, M., Taylor, S., Amziane, S. (2021). An investigation into the long-term carbonation of vegetal concretes containing a viscosity modifying agent. *Construction and Building Materials, 296,* 123765. DOI 10.1016/j.conbuildmat.2021.123765.

21.  Nozahic, V. (2012). *Vers une nouvelle démarche de conception des bétons de végétaux lignocellulosiques basée sur la compréhension et l'amélioration de l'interface liant/végétal : Application à des granulats de chènevotte et de tige de tournesol associés à un liant ponce/chaux* (*Ph.D. Thesis*). Université Blaise Pascal, Clermont-Ferrand II, France.

22.  Okino, Y. A. E., Souza, M. R., Santana, M. A. E., Alves, M. V. S., Sousa, M. E. et al. (2004). Cement-bonded wood particleboard with a mixture of eucalypt and rubberwood. *Cement Concrete Composites, 26(6),* 729–7340. DOI 10.1016/S0958-9465(03)00061-1.

23.  Romildo, D., Filho, T., Ghavami, K., England, G. L., Scrivener, K. (2003). Development of vegetable fibre-mortar composites of improved durability. *Cement Concrete Composites, 25(2),* 185–196. DOI 10.1016/S0958-9465(02)00018-5.

24.  Merzoud, M., Sellami, A., Gouasmia, A., Benazzouk, A., (2015). Effet du traitement des fibres de diss sur le comportement mécanique des composites cimentaires. *Conférence Internationale Francophone NoMaD 2015 (Nouveau Matériaux et Durabilité)*, LGCGE-Ecole des Mines de Douai, Lille Nord de France, France.

25.  Dabbaghi, F., Sadeghi-Nik, A., AliLibre, N., Nasrollahpour, S. (2021). Characterizing fiber reinforced concrete incorporating zeolite and Metakaolin as natural pozzolans. *Structures, 34,* 2617–2627. DOI 10.1016/j.istruc.2021.09.025.

26.  Askarian, M., Fakhretaha Aval, S., Joshaghani, A. (2018). A comprehensive experimental study on the performance of pumice powder in self-compacting concrete (SCC). *Journal of Sustainable Cement-Based Materials, 7(6),* 340–356. DOI 10.1080/21650373.2018.1511486.

27.  Vahabi, M. Y., Tahmouresi, B., Mosavi, H., Fakhretaha Aval, S. (2021). Effect of pre-coating lightweight aggregates on the self-compacting concrete. *Structural Concrete, 23(4),* 1–12. DOI 10.1002/suco.202000744.

28.  Sadeghi-Nik, A., Berenjian, J., Alimohammadi, S., Lotfi-Omran, O., Sadeghi-Nik, A. et al. (2019). The effect of recycled concrete aggregates and metakaolin on the mechanical properties of self-compacting concrete containing nanoparticles. *Iranian Journal of Science and Technology, Transactions of Civil Engineering, 43(1),* 503–515, DOI 10.1007/s40996-018-0182-4.

29.  Cerny, R., Kunca, A., Tydlitat, V., Drchalova, J., Rovnanikova, P. (2006). Effect of pozzolanic admixtures on mechanical, thermal and hygric properties of lime plasters. *Construction and Building Materials, 20(10),* 849–857. DOI 10.1016/j.conbuildmat.2005.07.002.

30.  CERADEL, ARGICALTM–M 1000. Metakaolin (2014). https://www.ceradel.fr/fr/matieres-premieres-de-base/15854-metakaolin-argical-m1000-25kg.html.

31.  Standard, EN 196-1 (2005). Methods of testing cement. *Determination of Strength Properties*.

32.  Wei, J., Meyer, C. (2015). Degradation mechanisms of natural fiber in the matrix of cement composites. *Cement and Concrete Research, 73,* 1–16. DOI 10.1016/j.cemconres.2015.02.019.

33.  Akhavan, A., Catchmark, J., Rajabipour, F. (2017). Ductility enhancement of autoclaved cellulose fiber reinforced cement boards manufactured using a laboratory method simulating the Hatschek process. *Construction and Building Materials, 135,* 251–259. DOI 10.1016/j.conbuildmat.2017.01.001.

34. Ballesteros, J. E. M., Mármol, G., Filomeno, R., Rodier, L., Savastano Jr., H. et al. (2019). Synergic effect of fiber and matrix treatments for vegetable fiber reinforced cement of improved performance. *Construction and Building Materials, 205,* 52–60. DOI 10.1016/j.conbuildmat.2019.02.007.

35. Deng, M., Han, J., Liu, H., Qin, M., Liang, X. (2015). Analysis of compressive toughness and deformability of high ductile fiber reinforced concrete. *Advanced in Materials Science and Engineering, 2015,* 1–7. DOI 10.1155/2015/384902.